Proc. Natl. Acad. Sci. USA
Vol. 91, pp. 12785–12789, December 1994
Physiology

Sodium channel mutations in paramyotonia congenita exhibit similar biophysical phenotypes *in vitro*

(myotonia/periodic paralysis/inactivation/electrophysiology)

NAIBO YANG†, SEN JI‡, MING ZHOU§, LOUIS J. PTÁČEK¶, ROBERT L. BARCHI‡, RICHARD HORN†, AND ALFRED L. GEORGE, JR.§

†Department of Physiology, Jefferson Medical College, Philadelphia, PA 19107; ‡Department of Neuroscience and the David Mahoney Institute of Neurological Sciences, University of Pennsylvania School of Medicine, Philadelphia, PA 19104; ¶Departments of Neurology and Human Genetics, University of Utah School of Medicine, Salt Lake City, UT 84132; and §Departments of Medicine and Pharmacology, Vanderbilt University School of Medicine, Nashville, TN 37232-2372

Communicated by James M. Sprague, September 15, 1994 (received for review July 1, 1994)

ABSTRACT **Mutations in the skeletal muscle voltage-gated Na^+ channel α-subunit have been found in patients with two distinct hereditary disorders of sarcolemmal excitation: hyperkalemic periodic paralysis (HYPP) and paramyotonia congenita (PC). Six of these mutations have been functionally expressed in a heterologous cell line (tsA201 cells) using the recombinant human skeletal muscle Na^+ channel α-subunit cDNA hSkM1. PC mutants from diverse locations in this subunit (T1313M, L1433R, R1448H, R1448C, A1156T) all exhibit a similar disturbance in channel inactivation characterized by reduced macroscopic rate, accelerated recovery, and altered voltage dependence. PC mutants had no significant abnormality in activation. In contrast, one HYPP mutation studied (T704M) has a normal inactivation rate but exhibits shifts in the midpoints of steady-state activation and inactivation along the voltage axis. These findings help to explain the phenotypic differences between HYPP and PC at the molecular and biophysical level and contribute to our understanding of Na^+ channel structure and function.**

Sodium channels are integral membrane proteins that exist in most excitable cells and are primarily responsible for the rapid depolarization characterizing the initial phase of an action potential (1). In skeletal muscle, Na^+ channels are essential for the propagation of action potentials along the muscle fiber surface and into the t-tubular system, triggering events that ultimately lead to contraction. Functional disturbances in muscle Na^+ channels are associated with unusual disease phenotypes generally categorized as the periodic paralyses and nondystrophic myotonias (2).

Paramyotonia congenita (PC) is a rare, autosomal dominant hereditary disease characterized by painless stiffness (myotonia) of voluntary muscles that occurs upon exposure to cold or following strenuous exercise (3). The disorder is clinically heterogeneous, and some patients exhibit episodic weakness and other features resembling another rare disorder, hyperkalemic periodic paralysis (HYPP). The clinical features of both PC and HYPP can be attributed to abnormal skeletal muscle membrane excitability, and symptoms can be correlated with either sarcolemmal hyperexcitability or inexcitability. In HYPP, the dominant clinical presentation is that of episodic muscle weakness or paralysis. Paralysis in this setting occurs concomitantly with a failure of the sarcolemma to initiate and conduct action potentials (inexcitability) (4). In contrast, PC patients primarily have symptoms of sarcolemmal hyperexcitability, with repetitive muscle action potentials that lead to muscle stiffness or myotonia.

The publication costs of this article were defrayed in part by page charge payment. This article must therefore be hereby marked "*advertisement*" in accordance with 18 U.S.C. §1734 solely to indicate this fact.

Electrophysiological evidence exists for a functional defect in the skeletal muscle Na^+ channel in patients with both HYPP and PC (4–7), and recent genetic studies have confirmed that HYPP and PC are allelic disorders of the skeletal muscle voltage-gated sodium channel α-subunit gene (*SCN4A*, 17q23.1-q25.3) (8–10). There have been 14 missense *SCN4A* mutations found in patients with either HYPP or PC; at least five are associated with a typical PC phenotype (11–17). Many of these identified mutations occur in regions of the Na^+ channel protein for which little or no structure–function correlation exists. Therefore, the relationship between these various genotypes and specific phenotypes is not immediately obvious.

To improve our understanding of these diseases we have studied six of these *SCN4A* mutations using the recombinant human skeletal muscle Na^+ channel (hSkM1) (18) expressed heterologously in a mammalian cell line. We find that all of the PC mutants exhibit similar changes in channel inactivation and that these changes are distinct from those that characterize the *in vitro* behavior of the expressed HYPP mutation. These observations provide solid evidence that the biophysical behavior of Na^+ channel alleles that cause PC differs from that of HYPP mutations.

MATERIALS AND METHODS

Construction and Expression of hSkM1 Mutants. Site-directed mutagenesis was performed using the Altered Sites mutagenesis system employing the plasmid vector pSELECT (Promega) as described (19). For creation of mutants A1156T and T1313M, an additional pSELECT-hSkM1 construct was made by directionally subcloning a 1564-bp *Sac* I/*Hin*dIII fragment (nt 2488–4051) of wild-type (WT) hSkM1 into the vector in the antisense orientation, and single-stranded DNA was rescued using R408 helper phage. For T704M, a 1909-bp *Bam*HI/*Sph* I fragment (nt 327–2235) was subcloned into the vector. Mutagenic oligonucleotides were as follows: A1156T, 5′-GCCCTCCTAGGCACCATCCCCTCCA-3′; T1313M, 5′-ACCTCTTTATGATGGAGGAACAGA-3′; L1433R, 5′-GATCAGGTCAGAGCGGGCAAGGCCCAC-3′; T704M, 5′-GGGTAACCTGATGCTGGTGCTGGC-3′; R1448H and R1448C were as described (19). All mutations were verified by dideoxynucleotide sequencing. Following mutagenesis, full-length mutant hSkM1 constructs were assembled in the mammalian expression vector pRc/CMV, and introduced into tsA201 cells by transient transfection (calcium phosphate precipitation method) as described (19). Cells were used for recording 24–60 hr after transfection.

Abbreviations: HYPP, hyperkalemic periodic paralysis; PC, paramyotonia congenita; WT, wild-type.

Electrophysiology. Standard whole cell recordings were obtained as described (19). We compensated 80% of the series resistance, which was always <3 MΩ. The series resistance errors were <4 mV. Patch electrodes contained (in mM) 35 NaCl, 105 CsF, 10 EGTA, and 10 Cs-Hepes (pH 7.4). The bath contained 150 NaCl, 2 KCl, 1.5 $CaCl_2$, 1 $MgCl_2$, and 10 Na-Hepes (pH 7.4). The data were filtered at 5 kHz and acquired using the program PCLAMP (Axon Instruments, Foster City, CA). Solution components were obtained from Sigma. Temperature was controlled by a Peltier unit using a TC-10 controller (Dagan Instruments, Minneapolis). Except where indicated, currents were measured at 21–22°C.

Whole cell data were analyzed by a combination of PCLAMP programs and SIGMAPLOT (Jandel, San Rafael, CA). Steady-state inactivation curves were fit to the equation $I/I_{max} = 1/\{1 + \exp[\delta_i F(V-V_{0.5})/RT\}$, where I_{max} is the current measured at the most negative prepulse potential (usually −140 mV), $V_{0.5}$ is the midpoint of the curve, δ_i is the slope factor, and RT/F = 25 mV. A Boltzmann curve was also fit to conductance–voltage curves obtained from peak current after a depolarization. Recovery from inactivation was fit to a single exponential decay, and the time constants at each recovery potential were fit to $\tau(V) = \tau(0) * \exp(\delta_r VF/RT)$, where δ_r is the slope of the curve and $\tau(0)$ is the time constant for recovery at 0 mV. Each experiment was performed on four to six cells, and the data are presented as mean ± SEM. Two independent clones for each mutant were characterized to decrease the possibility that the observed effects were due to inadvertent mutations.

RESULTS

PC Mutations Slow Na^+ Channel Inactivation. WT hSkM1 Na^+ channels and five PC mutants constructed in the hSkM1 background were expressed transiently in tsA201 cells and the resulting Na^+ currents were examined by patch clamp electrophysiology in the whole cell configuration. Fig. 1 shows sodium currents obtained by whole cell recording for these six alleles. The currents from all clones show a typical pattern of rapid voltage-dependent activation followed by inactivation. However, all of the PC mutant channel currents differed from WT in showing variable slowing in channel inactivation.

Normalized plots of peak current vs. membrane potential are superimposable for all six clones (Fig. 2*A*), suggesting that the voltage dependence of activation is unaffected by PC mutations. The kinetics of activation are also normal in the PC mutants. Superimposed scaled plots of the inward current at −10 mV for each clone show the striking effect of PC mutations on inactivation with little change in the kinetics of activation (Fig. 2*B*). A similarity in activation time course for WT and PC mutants was obtained at all membrane potentials, as measured by the half-time from the onset of the depolarization to the time of the peak current (Fig. 2*C*).

We quantified the slowing of inactivation for PC mutants by fitting the decay of sodium current, after a depolarizing voltage step, to a single exponential function with a time constant, τ_h. In general, a single exponential provided a good fit to the data, and the currents decayed to zero during sufficiently long depolarizations. These time constants are plotted in Fig. 3*A* as a function of membrane potential. All PC mutants had τ_h values significantly greater than those observed in the WT over the entire voltage range from −40 to +80 mV.

The voltage dependence of steady-state inactivation for the five PC mutants is also significantly altered (Fig. 3*B*). Table 1 shows that this voltage dependence, as indicated by the slopes obtained from Boltzmann curves fit to the data, decreases in the following order: WT > T1313M > A1156T > R1448H > L1433R > R1448C. Furthermore, mutants R1448H, L1433R, and R1448C exhibit large shifts in the midpoints of steady-state inactivation, when compared with the WT (Fig. 3*B*; Table 1). The midpoints are shifted in the hyperpolarizing direction for the two mutants in the S4 segment of domain 4 (S4/D4), R1448H and R1448C, and in the depolarizing direction for the S3/D4 mutant L1433R. These differences imply that a single mechanism may not explain the alterations in channel gating characteristics of PC mutants.

PC Mutations Accelerate Recovery from Inactivation. Despite having slowed inactivation, all of the PC mutants that we examined had a faster rate of recovery from inactivation

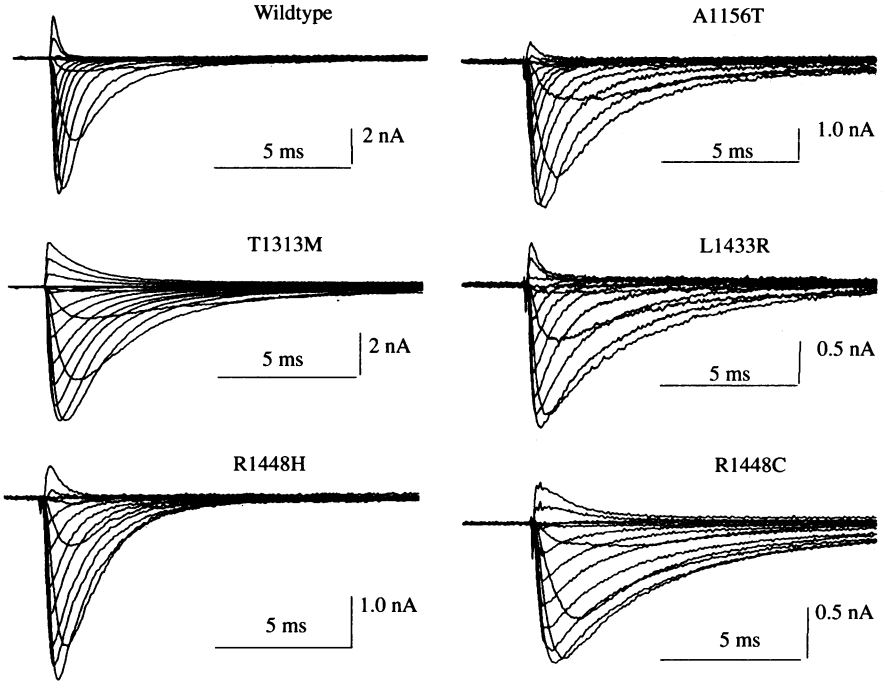

FIG. 1. Effect of PC mutations on macroscopic sodium currents. Cells were held at −100 mV and activated by depolarizations in 10-mV increments from −60 mV to +80 mV.

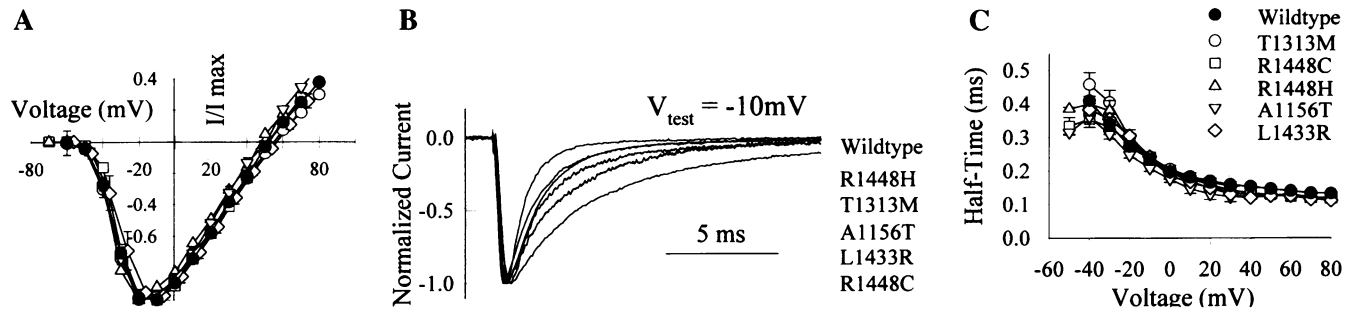

FIG. 2. Activation in PC mutants. (*A*) Normalized current–voltage relationships for the peak currents for WT and PC mutations. (*B*) Superimposed currents at −10 mV, normalized to the same peak value. The clones are listed in order of their effects on the rate of inactivation, with WT being fastest and R1448C the slowest at this voltage. (*C*) Half-time for activation vs. membrane potential.

than the WT channels (Fig. 3*C*). The voltage dependence of the recovery rate was also affected in the PC mutants. The slopes of the regression lines of the semilogarithmic plot of Fig. 3*C* (expressed as an equivalent charge; see *Materials and Methods*) are a direct measurement of the voltage dependence of the recovery rate. Table 1 shows that this voltage dependence has the same relative order among the six mutants as we observed for steady-state inactivation. The reduction in voltage dependence is most severe in mutants R1448H, L1433R, and R1448C. These three mutants are all in domain 4 and are located near the extracellular surface of the channel, according to a standard topological interpretation of the structure of the sodium channel (20). This raises the possibility that R1448 and L1433 are located within structures that are important for inactivation.

Temperature Sensitivity of PC Mutations. One of the clinical features of PC is the exacerbation of muscle stiffness by cold, and many investigators assumed that the corresponding Na^+ channel mutations would prove to be temperature sensitive (15). We previously found little difference between the temperature dependence of τ_h in WT and that observed in the PC mutants at residue R1448 for temperatures between 14°C and 30°C (19). We obtained similar measurements for the PC mutant T1313M and again found little difference from the WT over this temperature range (data not shown).

Biophysical Differences Between PC and HYPP. Two HYPP mutations, T704M and M1592V, have been constructed in rSkM1, the rat homolog of hSkM1, and expressed transiently in mammalian cells by other investigators (21, 22). The currents generated by these HYPP mutations differ substantially from those we describe here for PC mutants. One report showed a small noninactivating component of macroscopic sodium current after a depolarization (21), whereas the other report emphasized a 10- to 15-mV hyperpolarizing shift in the peak current–voltage relationship (22). Neither study reported significant changes in the time constants for fast inactivation. In contrast, the PC mutants we studied all have voltage dependences of activation indistinguishable from WT and show a pronounced slowing of fast inactivation. However, our data were obtained with the human muscle Na^+ channel (hSkM1) rather than the rat muscle channel used in the above studies. We therefore constructed the HYPP mutant T704M in hSkM1 and examined its properties under the same conditions as above, to test if PC and HYPP mutations truly produce distinct functional abnormalities in hSkM1.

Fig. 4*A* shows a family of sodium currents from the HYPP mutant T704M. The peak current–voltage relationship of these currents is compared with the WT in Fig. 4*B*. These data show two properties consistent with the previous studies using this mutation in rSkM1, a small increase in noninactivating current, especially seen at positive voltages in our experiments, and a hyperpolarizing shift in the peak current–voltage relationship (21, 22). When compared with WT, T704M showed no difference in τ_h (Fig. 4*C*) or recovery from inactivation (data not shown). However, in contrast with the

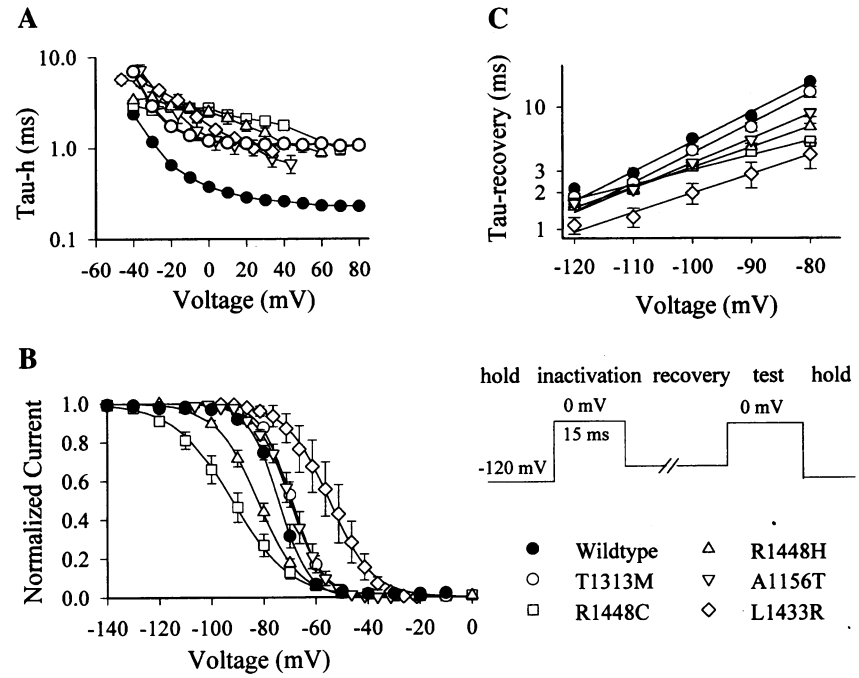

FIG. 3. Inactivation in PC mutants. (*A*) Time constants of inactivation vs. voltage for currents activated by step depolarizations. The decay of current after the peak was well fit by a single exponential relaxation with a time constant τ_h. All mutations show a significant increase in τ_h, as seen in the sodium currents of Fig. 1. (*B*) Steady-state inactivation at −10 mV induced by 500-ms prepulses at the indicated voltages. Holding potential, −120 mV. The curves were fit to the equation in *Materials and Methods*. The best-fit midpoints and slopes are listed in Table 1. (*C*) Recovery time constants vs. recovery membrane potential. Voltage protocol is shown below the plot. Cells were held at −120 mV and inactivated with a 15-ms, 0-mV prepulse. The time course of recovery was well fit by a single exponential. The time constants of recovery were fit to the equation in *Materials and Methods*. The slopes are given in Table 1.

Table 1. Voltage dependence of inactivation

Sample	Recovery		Steady state	
	δ_r, e_0	$\tau(0)$, s	δ_i, e_0	$V_{0.5}$, mV
WT	1.40 ± 0.03	1.43 ± 0.19	5.05 ± 0.07	−75.5 ± 0.8
T1313M	1.40 ± 0.04	1.23 ± 0.31	4.75 ± 0.13	−66.8 ± 1.2
A1156T	1.16 ± 0.08	0.42 ± 0.13	3.93 ± 0.07	−69.9 ± 0.1
R1448H	0.96 ± 0.02	0.15 ± 0.02	3.12 ± 0.08	−82.3 ± 0.8
L1433R	0.86 ± 0.08	0.09 ± 0.04	3.01 ± 0.07	−55.5 ± 0.3
R1448C	0.71 ± 0.02	0.05 ± 0.002	2.27 ± 0.10	−92.0 ± 3.4

Symbols and equations defined in *Materials and Methods*. The data for steady-state inactivation for R1448H and R1448C were obtained from a previous study (19).

results of Cummins *et al.* (22), steady-state inactivation in T704M was shifted 12.8 mV in the depolarizing direction (Fig. 4*D*). Thus, it would seem that this mutation produces a more severe phenotype when expressed in hSkM1 than in rSkM1. The combination of a 9.1-mV hyperpolarizing shift of activation with a depolarizing shift of inactivation (Fig. 4*D*) creates a range of voltages (−65 to −30 mV) over which a steady-state sodium current will flow.

DISCUSSION

Understanding the molecular basis for gating of ion channels by membrane potential has been the subject of intense investigation. A unique opportunity now exists to examine previously unexplored regions of the voltage-gated Na^+ channel by using two unusual genetic diseases of muscle, PC and HYPP, as models for channel dysfunction. In these two distinct, but related, disorders of muscle membrane excitability, mutations in the gene encoding the skeletal muscle Na^+ channel α-subunit disturb gating of the channel in unique ways.

In our experiments using the human muscle Na^+ channel hSkM1, the HYPP mutant T704M shifts the midpoints of steady-state activation and inactivation along the voltage axis without affecting the rate or voltage dependence of either process. These functional abnormalities can lead to persistent Na^+ current at voltages where the activation and inactivation curves overlap (Fig. 4*D*). The occurrence of this "window current" will tend to cause depolarization of skeletal muscle cells in HYPP patients. In contrast, Na^+ channel mutations found in PC exhibit normal activation kinetics but share three characteristic disturbances in inactivation: (*i*) reduced rate and voltage dependence of inactivation, (*ii*) altered voltage dependence of steady-state inactivation, and (*iii*) increased rate and decreased voltage dependence of recovery from inactivation.

Alterations in either the kinetic or the steady-state properties of inactivation may have significant effects on muscle excitability. The kinetic effects seen with PC mutations, a decreased rate of inactivation and an increased rate of recovery from inactivation, would increase excitability during and following action potentials. By contrast, the steady-state properties of inactivation will determine the number of Na^+ channels available to open during a depolarization. It is in this regard that the PC mutants differ dramatically among one another. Our data show hyperpolarizing shifts in steady-state inactivation for mutations of R1448 but depolarizing shifts for all other mutants, especially L1433R (Fig. 3*B*; Table 1). However, individuals with either the R1448 or the L1433 mutation have a similar PC phenotype (12, 13). Thus, the final clinical expression of these mutations seems unrelated to the direction and magnitude of the shifts they produce in steady-state inactivation. Since all of the PC mutations studied produce similar abnormalities in the kinetics of inactivation, the kinetic effects are likely to be the most important in determining phenotype.

The hyperpolarizing shifts in steady-state inactivation for R1448 mutants cannot be explained by a slow inactivation of the channel during the 500-ms prepulse we used for measuring steady-state inactivation, because similar experiments with R1448C using 25-ms prepulses produced data with the same midpoint as we observed in Fig. 3*B* (data not shown). A possible explanation for this is that the rate of entry into an inactivated state is faster for these mutants than WT at potentials more negative than −60 mV. This is the expected result of the extrapolation of τ_h vs. voltage curves (Fig. 3*A*) to voltages more negative than −40 mV. For example, the τ_h of R1448C is almost completely voltage independent below 0 mV (see figure 2B in ref. 19), whereas τ_h for WT increases strongly with hyperpolarization (Fig. 3*A*). Therefore, even though R1448C channels recover faster from inactivation than WT channels at voltages more hyperpolarized than −80

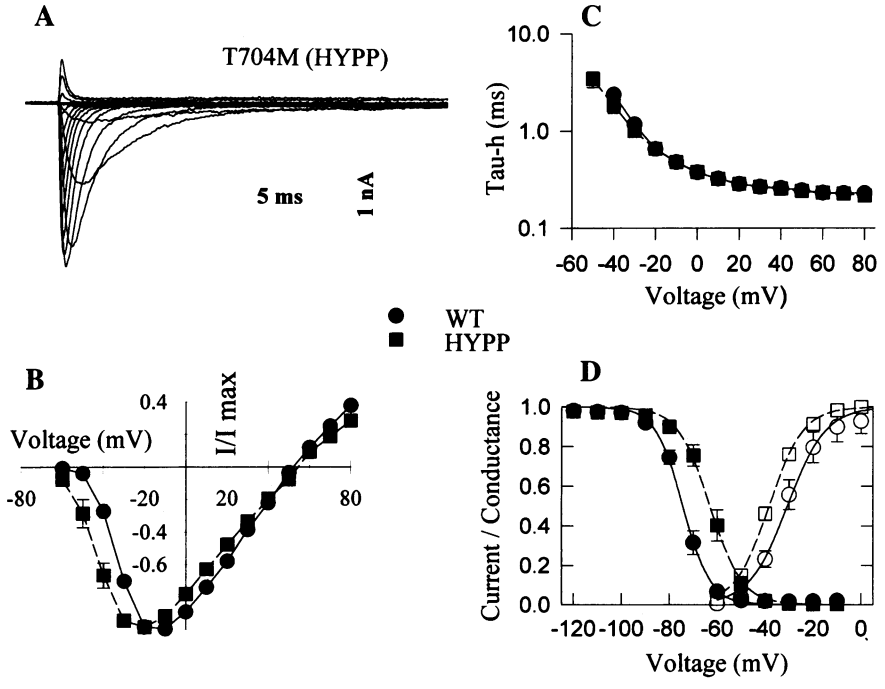

FIG. 4. Sodium currents of T704M. (*A*) Cells were held at −100 mV and activated by depolarizations in 10-mV increments from −60 to +80 mV. (*B*) Normalized current–voltage relationships for the peak currents for WT and T704M. (*C*) τ_h vs. voltage for WT and T704M. (*D*) Steady-state inactivation (solid symbols) and normalized conductance–voltage (G–V) curves (open symbols) for WT and T704M. Both curves were fit by a Boltzmann relationship. The midpoint and slope of the inactivation curve for T704M are −62.7 ± 2.1 mV and 5.05 ± 0.07e_0. The midpoint and slope of the G–V curve for the WT are −29.3 ± 3.9 mV and 3.05 ± 0.70e_0; for T704M these values are −38.4 ± 1.2 mV and 3.59 ± 0.09e_0.

mV (Fig. 4*C*), the entry into inactivated states will be much more frequent for R1448C than WT and hence a greater degree of steady-state inactivation at these voltages.

The PC mutations that we studied all affect channel inactivation. We speculate that they either alter the structure of the inactivation gate or its receptor or modify the kinetics of inactivation by affecting conformational transitions elsewhere in the channel protein. The inactivation gate has been postulated to be the cytoplasmic linker between D3 and D4 (23, 24). One of the PC mutants, T1313M, is in this linker and its neighboring residues (isoleucine, phenylalanine, methionine) are known to play a critical role in fast inactivation (25). Of the other four PC mutations, one, A1156T, is located in the cytoplasmic loop between S4 and S5 in D3. The corresponding segment in voltage-gated potassium channels is believed to be part of the receptor for the inactivation gate (26). The remaining three mutations are located at a distance from either the inactivation gate or its putative receptor in current models of Na^+ channel structure (L1433R, D4/S3; R1448H and R1448C, D4/S4). One possibility that would account for the similar phenotype of these mutants is that, through allosteric effects, they indirectly modify the conformation of the gate or its receptor. Another hypothesis is that these mutants affect a part of the molecule that must undergo a critical conformation change during the steps leading to gate–receptor interaction. Such mutations might have a profound effect on the macroscopic rates of channel inactivation without directly affecting the binding affinity of the gate for its receptor site on the cytoplasmic surface of the protein. Finally, since the Na^+ channel β_1 subunit is known to have significant effects on hSkM1 inactivation (27), mutations that disrupt the association of α and β_1 subunits could produce slowed inactivation similar to that observed for PC mutants. We feel this is not a likely explanation for our data since absence of β_1 subunit would result in slowed recovery from inactivation as well (28), not accelerated recovery as observed with PC mutations. However, mutations that affect the interaction of α and β_1 subunits in a more specific fashion might produce phenotypes similar to those seen for the PC mutants described here.

This work was supported by National Institutes of Health Grants NS32387, AR41691, NS18013, and HD00940 and by a grant from the Muscular Dystrophy Association (R.L.B.). A.L.G. is a Lucille P. Markey Scholar, and this work is supported in part by a grant from the Lucille P. Markey Charitable Trust.

1. Catterall, W. A. (1992) *Physiol. Rev.* **72,** Suppl., S15–S48.
2. Barchi, R. L. & Furman, R. E. (1992) in *Diseases of the Nervous System*, eds. Asbury, A. K., Mckhann, G. M. & McDonald, W. I. (Saunders, Philadelphia), pp. 146–163.
3. Griggs, R. C. (1977) *Adv. Neurol.* **17,** 143–159.
4. Rüdel, R. & Lehmann-Horn, F. (1985) *Physiol. Rev.* **65,** 310–356.
5. Lehmann-Horn, F., Rüdel, R., Ricker, K., Lorkovic, H., Dengler, R. & Hopf, H. C. (1983) *Muscle Nerve* **6,** 113–121.
6. Lehmann-Horn, F., Rüdel, R. & Ricker, K. (1987) *Muscle Nerve* **10,** 633–641.
7. Cannon, S. C., Brown, R. H. & Corey, D. P. (1991) *Neuron* **6,** 619–626.
8. Fontaine, B., Khurana, T. S., Hoffman, E. P., Bruns, G. A. P., Haines, J. L., Trofatter, J. A., Hanson, M. P., Rich, J., McFarlane, H., Yasek, D. M., Romano, D., Gusella, J. F. & Brown, R. H. (1990) *Science* **250,** 1000–1002.
9. Ptáček, L. J., Trimmer, J. S., Agnew, W. S., Roberts, J. W., Petajan, J. H. & Leppert, M. (1991) *Am. J. Hum. Genet.* **49,** 851–854.
10. Ebers, G. C., George, A. L., Barchi, R. L., Kallen, R. G., Ting-Passador, S. S., Lathrop, M., Beckmann, J., Hahn, A. F., Brown, W. F., Campbell, R. & Hudson, A. J. (1991) *Ann. Neurol.* **30,** 810–816.
11. Ptáček, L. J., George, A. L., Griggs, R. C., Tawil, R., Kallen, R. G., Barchi, R. L., Robertson, M. & Leppert, M. F. (1991) *Cell* **67,** 1021–1027.
12. Ptáček, L. J., George, A. L., Barchi, R. L., Griggs, R. C., Riggs, J. E., Robertson, M. & Leppert, M. F. (1992) *Neuron* **8,** 891–897.
13. Ptáček, L. J., Gouw, L., Kwiecinski, H., McMainis, P., Mendell, J. R., Barohn, R. J., George, A. L., Barchi, R. L., Robertson, M. & Leppert, M. F. (1993) *Ann. Neurol.* **33,** 300–307.
14. Rojas, C. V., Wang, J., Schwartz, L. S., Hoffman, E. P., Powell, B. R. & Brown, R. H. (1991) *Nature (London)* **354,** 387–389.
15. McClatchey, A. I., Van den Bergh, P., Pericak-Vance, M. A., Raskind, W., Verellen, C., McKenna-Yasek, D., Keshav, R., Haines, J. L., Bird, T., Brown, R. H. & Gusella, J. F. (1992) *Cell* **68,** 769–774.
16. McClatchey, A. I., McKenna-Yasek, D., Cros, D., Worthen, H. G., Kuncl, R. W., DeSilva, S. M., Cornblath, D. R., Gusella, J. F. & Brown, R. H., Jr. (1992) *Nat. Genet.* **2,** 148–152.
17. Ptáček, L. J., Tawil, R. & Griggs, R. C. (1994) *Neurology* **44,** A335 (abstr.).
18. George, A. L., Komisarof, J., Kallen, R. G. & Barchi, R. L. (1992) *Ann. Neurol.* **31,** 131–137.
19. Chahine, M., George, A. L. Jr., Zhou, M., Ji, S., Sun, W., Barchi, R. L. & Horn, R. (1994) *Neuron* **12,** 281–294.
20. Noda, M., Shimizu, S., Tanabe, T., Takai, T., Kayano, T., Ikeda, T., Takahashi, H., Nakayama, H., Kaknaoka, Y., Minamino, N., Kkangawa, K., Matsuo, H., Raftery, M. A., Hirose, T., Inayama, S., Hayashida, H., Miyata, T. & Numa, S. (1984) *Nature (London)* **312,** 121–127.
21. Cannon, S. C. & Strittmatter, S. M. (1993) *Neuron* **10,** 317–326.
22. Cummins, T. R., Zhou, J., Sigworth, F. J., Ukomadu, C., Stephan, M., Ptáček, L. J. & Agnew, W. S. (1993) *Neuron* **10,** 667–678.
23. Stühmer, W., Conti, F., Suzuki, H., Wang, X., Noda, M., Yahagi, N., Kubo, H. & Numa, S. (1989) *Nature (London)* **339,** 597–603.
24. Vassilev, P., Scheuer, T. & Catterall, W. A. (1989) *Proc. Natl. Acad. Sci. USA* **86,** 8147–8151.
25. West, J. W., Patton, D. E., Scheuer, T., Wang, Y., Goldin, A. L. & Catterall, W. A. (1992) *Proc. Natl. Acad. Sci. USA* **89,** 10910–10914.
26. Isacoff, E. Y., Jan, Y. N. & Jan, L. Y. (1991) *Nature (London)* **353,** 86–90.
27. Makita, N., Bennett, P. B., Jr., & George, A. L., Jr. (1994) *J. Biol. Chem.* **269,** 7571–7578.
28. Ji, S., Sun, W., George, A., Horn, R. & Barchi, R. (1994) *J. Gen. Physiol.* **104,** 625–643.